BIOCHEMISTRY
including biophysical chemistry & molecular biology

Article

pubs.acs.org/biochemistry

Environmental Pollutant Ozone Causes Damage to Lung Surfactant Protein B (SP-B)

Joanna M. Hemming,[†] Brian R. Hughes,[†] Adrian R. Rennie,[‡] Salvador Tomas,[†] Richard A. Campbell,[§] Arwel V. Hughes,[∥] Thomas Arnold,[⊥] Stanley W. Botchway,[#] and Katherine C. Thompson*[,†]

[†]Department of Biological Sciences and Institute of Structural and Molecular Biology, Birkbeck College, University of London, Malet Street, London WC1E 7HX, U.K.

[‡]Materials Physics, Department of Physics and Astronomy, Uppsala University, 75120 Uppsala, Sweden

[§]Institut Laue-Langevin, 71 Avenue des Martyrs, CS20156, 38042 Grenoble Cedex 09, France

[∥]ISIS Pulsed Neutron and Muon Source, STFC Rutherford Appleton Laboratory, Harwell Oxford, Didcot, Oxfordshire OX11 0QX, U.K.

[⊥]Diamond Light Source, Harwell Science and Innovation Campus, Didcot OX11 0DE, U.K.

[#]STFC, Lasers for Science Facility, Central Laser Facility, Research Complex at Harwell, STFC Rutherford Appleton Laboratory, Harwell Oxford, Didcot, Oxfordshire OX11 0FA, U.K.

Supporting Information

ABSTRACT: Lung surfactant protein B (SP-B) is an essential protein found in the surfactant fluid at the air−water interface of the lung. Exposure to the air pollutant ozone could potentially damage SP-B and lead to respiratory distress. We have studied two peptides, one consisting of the N-terminus of SP-B [SP-$B_{(1-25)}$] and the other a construct of the N- and C-termini of SP-B [SP-$B_{(1-25,63-78)}$], called SMB. Exposure to dilute levels of ozone (∼2 ppm) of monolayers of each peptide at the air−water interface leads to a rapid reaction, which is evident from an increase in the surface tension. Fluorescence experiments revealed that this increase in surface tension is accompanied by a loss of fluorescence from the tryptophan residue at the interface. Neutron and X-ray reflectivity experiments show that, in contrast to suggestions in the literature, the peptides are not solubilized upon oxidation but rather remain at the interface with little change in their hydration. Analysis of the product material reveals that no cleavage of the peptides occurs, but a more hydrophobic product is slowly formed together with an increased level of oligomerization. We attributed this to partial unfolding of the peptides. Experiments conducted in the presence of phospholipids reveal that the presence of the lipids does not prevent oxidation of the peptides. Our results strongly suggest that exposure to low levels of ozone gas will damage SP-B, leading to a change in its structure. The implication is that the oxidized protein will be impaired in its ability to interact at the air−water interface with negatively charged phosphoglycerol lipids, thus compromising what is thought to be its main biological function.

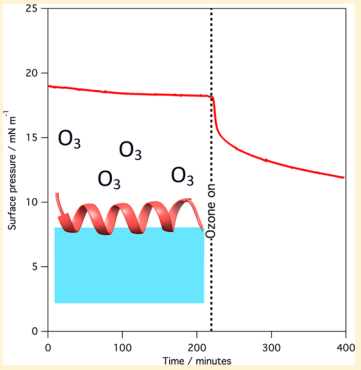

The air−water interface of the lung requires a layer of surfactant material to prevent alveolar collapse.[1] The exact composition of the surfactant material at the interface varies between species but contains mainly lipids, ∼90% by weight, and two hydrophobic proteins, surfactant protein B (SP-B) and surfactant protein C (SP-C), which make up the remaining 10%.[2] A range of lipids are required for correct respiratory function, and various types of phospholipids constitute around 80% by weight of lung surfactant and neutral lipids, mostly cholesterol, ∼10%. Approximately half the total phospholipid present in humans is the saturated lipid 1,2-dipalmitoyl-*sn*-glycero-3-phosphocholine (DPPC).[3] However, the condition of premature infants, and animals, born with an insufficiency of lung surfactant does not dramatically improve if they are treated with a surfactant of pure DPPC, whereas treatment with lipid mixtures or lipid/protein mixtures has been shown to be very successful.[4−7] The general consensus is that the other, mainly unsaturated, phospholipids present such as 1-palmitoyl-2-oleoyl-*sn*-glycero-3-phosphocholine (POPC) and its anionic analogue, 1-palmitoyl-2-oleoyl-*sn*-glycero-3-phosphoglycerol (POPG), are required to fluidize the otherwise fairly rigid DPPC monolayer and thus provide the required dynamical properties of the interfacial layer.[2] The two proteins directly associated with the air−water interface, SP-B and SP-C, interact with the lipids and are implicated in the transfer of lipids to and retention of lipids at the interface.[2] The presence of SP-B is vital for survival. Human infants born, at full term, without a working version of SP-B due to a genetic disorder do not survive.[8−11] Mice with the SP-B gene deleted from both chromosomes die within days of birth.[12] The presence of SP-C

Received: March 20, 2015
Revised: July 30, 2015
Published: August 13, 2015

DOI: 10.1021/acs.biochem.5b00308
Biochemistry 2015, 54, 5185−5197

SP-B FPIPLPYCWLCRALIKRIQAMIPKGALAVAVAQVCRVVPLVAGGICQCLAERYSVILLDTLLGRMLPQLVCRLVLRCSM

SMB FPIPLPYCWLCRALIKRIQAMIPKG_____GRMLPQLVCRLVLRCS

SP-$B_{(1-25)}$ FPIPLPYCWLCRALIKRIQAMIPKG

Figure 1. Primary structures of the full-length human protein SP-B (UniProt entry sp|P07988|201−279), N- and C-terminal construct SMB, and N-terminal peptide SP-$B_{(1-25)}$.

is less crucial, but a lack of SP-C is also linked to respiratory problems.[13]

Ozone is present as a secondary pollutant in ambient air. It has long been known that exposure to ozone, O_3, leads to respiratory problems, increased hospital admissions, and death.[14−16] What is not clear is the actual mechanism, or mechanisms, by which ozone exposure leads to respiratory problems. The surfactant at the air−water interface of the lung is one of the first lines of defense when humans are exposed to ozone present in ambient air. Several studies have attempted to investigate the effect of short- and longer-term ozone exposures *in vivo* on a pulmonary surfactant. Müller and co-workers[17] and Putman and co-workers[18] studied the surface tension of lung surfactant retrieved from rats after exposure to 0.8 ppm ozone for 2 and 12 h. The adsorption of the surfactant to the air−water interface after exposure to ozone was significantly slower, and the final surface tension reached was higher following exposure.

It is known that unsaturated lipids present at the air−water interface will react readily with ozone.[19−23] No reports of the exposure of proteins SP-B and SP-C to ozone have been published, but Kim et al. have reported a rapid reaction between a peptide composed of the first 25 amino acids of SP-B, known as SP-$B_{(1-25)}$, at the air−water interface of an aqueous droplet and high levels of gas-phase ozone.[24] Kim et al. studied the products of the reaction using field-induced droplet ionization mass spectrometry and reported that the oxidized product contained three more oxygen atoms than SP-$B_{(1-25)}$, which they deduced came from the oxidation of methionine to methionine sulfoxide and tryptophan to *N*-formylkynrenine. The signal-to-noise ratio for the product, SP-$B_{(1-25)}$ + 3O, was much lower than for the starting material, SP-$B_{(1-25)}$; hence, Kim et al. suggest that the oxidized form of SP-$B_{(1-25)}$ may be lost entirely from the interface, rationalized by the conversion of fairly hydrophobic residues into more hydrophilic species.

In this work, we have studied the effect of ozone exposure at the air−water interface on two truncated versions of SP-B, SP-$B_{(1-25)}$ and SP-$B_{(1-25,\ 63-78)}$, which is known as Super Mini B (SMB). SMB has been shown to better mimic the properties of full-length SP-B, compared to SP-$B_{(1-25)}$, although both SP-$B_{(1-25)}$ and SMB improve lung function in surfactant deficient animal models.[25,26] The sequences of the full-length human protein SP-B, SP-$B_{(1-25)}$, and SMB are shown in Figure 1.

The full-length protein SP-B is a small, 79-amino acid residue, 8.7 kDa protein. Although hydrophobic, at physiological pH, it carries a positive charge of ∼7, which is thought to be important for selective interaction with negatively charged lipids such as phosphoglycerols.[2] Peptides SMB and SP-$B_{(1-25)}$ carry positive charges of ∼7 and ∼4, respectively, at physiological pH. The seven cysteine residues in SP-B are all involved in disulfide bonds, three of which are intramolecular and the last of which is intermolecular to another SP-B monomer. A crystal or NMR structure of full-length protein SP-B has not yet been reported, but circular dichroism and FTIR experiments reveal approximately 40−50% α-helical content when in micelles and lipid bilayers.[27,28] A recent review by Olmeda et al. discusses the likely structure of SP-B in lipid membranes based on sequence homology with other proteins in the saposin family, all of which interact with lipids.[29] Structural studies have been performed on the peptide components of SP-B studied in this work, SP-$B_{(1-25)}$ and SMB. Gordon et al. studied the structure of SP-$B_{(1-25)}$ in POPG vesicles and found it to be predominantly α-helical; Kurutz and Lee reported that the shorter peptide SP-$B_{(11-25)}$ dissolved in methanol was α-helical, and Booth et al. studied the structure of C-terminal segment SP-$B_{(63-78)}$ in SDS micelles and found that it consisted of an amphipathic helix.[30−32] Shanmukh et al. reported that the secondary structure of the monomeric form of SP-$B_{(1-25)}$ at the air−water interface depended upon the surrounding environment.[33] The peptide had a predominantly α-helical structure when present as a pure film, a predominantly β-sheet secondary structure at the interface when present in 10 wt % mixtures with 4:1 DPPC/DOPG lipid mixtures, where DOPG is the unsaturated lipid 1,2-dioleoyl-*sn*-glycero-3-phosphoglycerol, but was predominantly α-helical when present at 1 wt % in a 4:1 DPPC/DOPG lipid mixture. Waring et al. and Sarker et al. studied a short version of SMB, SP-$B_{(8-25,63-78)}$, and found the structure was consistent with two linked amphipathic α-helices and contained two intramolecular disulfide bonds.[34,35] There have been a few neutron reflectometry studies of SP-B at the air−water interface[36,37] and an X-ray reflectometry study of SP-$B_{(1-25)}$ at the air−water interface,[38] but no one has used these methods to follow changes to SP-B upon its exposure to gas-phase ozone.

In this work, we have used a variety of analytical methods to study the effects of exposure of SP-$B_{(1-25)}$ and SMB at the air−water interface to low levels of gas-phase ozone. We have investigated the behavior of monolayers containing just the peptides and also mixed monolayers containing both a peptide and a lipid component. The lipids studied were the most abundant lung lipid, DPPC, and the anionic lipid POPG. POPG was chosen as it is the most abundant anionic lipid in adult human lung surfactant,[39] and it is believed that the interaction of SP-B with anionic lipids is important for lung function.[2] Although anionic lipids in the lung are predominantly unsaturated,[39] to selectively examine changes in the interaction of SMB to the anionic headgroup of lipids upon oxidation of SMB we also performed studies in which SMB and the saturated anionic lipid DPPG were exposed to ozone.

MATERIALS AND METHODS

The SP-$B_{(1-25)}$ and SMB peptides were supplied by Peptide Protein Research Ltd. The peptides were synthesized using standard Fmoc chemistry with a stated purity of >98%. The SMB peptide was subjected to air oxidation to produce the folded form with two internal disulfide bonds (Cys8−Cys49 and Cys11−CysC34), equivalent to the internal disulfides formed by full-length SP-B, as reported previously.[25] All lipids used were supplied by Avanti Polar Lipids (Alabaster, AL).

DOI: 10.1021/acs.biochem.5b00308
Biochemistry 2015, 54, 5185−5197

Other reagents were obtained from commercial sources and of ≥98% purity. The chloroform was stabilized with 0.5−1% ethanol.

The reaction between gas-phase ozone and monolayers of SP-$B_{(1-25)}$ and SMB either as pure peptide films or as mixtures with phospholipids at the air−water interface was studied under various conditions. In general, monolayers were prepared on an aqueous 50 mM, pH 7, sodium phosphate-buffered subphase contained in a PTFE-lined Langmuir trough (Nima Technology) housed in an environmental chamber to contain the ozone. The monolayers were prepared by slowly adding solutions of the peptide, or the peptide/lipid mixture, to the surface of the aqueous subphase using a Hamilton syringe. The peptide solutions were prepared as 0.2 mg mL^{-1} peptide dissolved in a 5:1 (v/v) chloroform/methanol solvent; lipid mixtures were prepared as 1 mg mL^{-1} lipid in chloroform. Binary mixtures of peptide and lipids were prepared by mixing the required amounts of each solution. After the addition of the peptide or peptide/lipid mixtures to the surface of the subphase, the solvent was allowed to evaporate under a flow of oxygen gas before the experiments were started. The experiments were performed by continuously flowing a dilute (varied between ∼0.1 and 3 ppm) mixture of ozone in oxygen (BOC, ≥99.5%) at a constant flow rate of 1 or 2 L min^{-1} through the chamber. The ozone was generated by passing dry oxygen through a commercial ozone generator (UVP) that generated ozone from the photolysis of molecular oxygen.

Surface Pressure Measurements. The surface pressure, equal to the difference between the surface tension of the gas−water interface of pure water and that of the interface under study, was measured as the monolayer films of the peptides and peptide/lipid mixtures were held at a constant area and exposure to gas-phase ozone. The surface pressure was measured using a Wilhelmy plate made from Whatman chromatography grade filter paper. Experimental constraints meant that relatively low surface pressures (<40 mN m^{-1}) were used in all cases.

HPLC and SDS−PAGE Analysis. After exposure of monolayers of SP-$B_{(1-25)}$ and SMB at the air−water interface to ozone, the reaction products were recovered by extraction with chloroform. The chloroform was then removed by using a rotary evaporator, and then the product was dried under a flow of dry nitrogen gas for several hours. The presence of cleaved peptide reaction products, or other products, was investigated by performing (i) SDS−PAGE analysis of the SP-$B_{(1-25)}$ samples and (ii) HPLC analysis of both the SP-$B_{(1-25)}$ and SMB samples recovered after reaction.

For the SDS−PAGE experiments, the peptide material recovered following removal of the chloroform was redissolved in 50 μL of a loading buffer [Tris (pH 6.8) and 2% SDS with 0.1 M reducing agent dithiothreitol (DTT), when stated] and run on a 18% acrylamide/bis(acrylamide) (19:1) resolving gel and a 5% (29:1) stacking gel, with a tricine buffer system as described by Schägger.[40] After electrophoresis, the peptides were fixed using 5% glutaraldehyde and the gel was stained using silver staining, which revealed the position of the peptides in the gel.[40] Bio-Rad Polypeptide SDS-PAGE Molecular Weight Standard was prepared in the same loading buffer with DTT and loaded into the gel to provide a molecular weight standard. A sample of the peptide dissolved directly in the loading buffer was run for comparison with material that had been extracted from the air−water interface. A control run was performed where the trough was filled with buffer only and treated with chloroform as described above. Extraction and analysis of SP-$B_{(1-25)}$ monolayers in this way were straightforward, and the results are presented. However, SMB transfers less readily into the aqueous SDS−PAGE buffer medium than SP-$B_{(1-25)}$, and we were unable to obtain consistent transfer of the peptide to the gel; thus, no results are presented.

For the HPLC analysis, the material recovered after removal of the chloroform was dissolved in a small quantity of ethanol. The material extracted in this way was analyzed using HPLC with a C5 column (Jupiter 5 μm C5 300 Å, 250 × 4.6 mm, Phenomenex) and solvent of (i) ethanol and water [3:1 (w/w)] or (ii) propan-2-ol, both with 0.1% trifluoracetic acid, with a gradient of 0 to 50% solvent ii over 40 min with a flow rate of 0.5 mL min^{-1}, and monitoring the absorption of the eluent at 254 nm.

Fluorescence Microscopy Measurements. Monolayers of SMB were formed on an aqueous subphase contained in a plastic Petri dish with a glass bottom (MatTek). Fluorescent lifetime images, and maximal fluorescence intensities, were recorded using a setup described previously.[41] Briefly, a custom-built two-photon microscope was constructed using scanning XY galvanometers (GSI Lumonics Ltd.). A diode-pumped (Verdi V18) titanium sapphire (Mira F900) operating at 700−980 nm was used to pump an optical parametric oscillator (OPO, APE-Coherent, GmbH, Berlin, Germany) to generate a laser wavelength at 590 nm, with a pulse width of 180 fs and a repetition rate of 76 MHz. The laser beam was focused to a diffraction-limited spot using a water-immersion ultraviolet corrected objective (Nikon VC, 60×, NA 1.2) and specimens were illuminated on the microscope stage of a modified Nikon TE2000-U instrument with UV-transmitting optics. The tryptophan residue of SMB was excited using two-photon excitation. The intensity and lifetime of the emitted fluorescence light (∼380 nm) were recorded before and after the surface was exposed briefly to a 3 ppm source of ozone, flowing at a rate of 1 L min^{-1}.

Fluorescence emission was collected without descanning, bypassing the scanning system, and passed through a narrowband interference (UG11, Comar) filter used to isolate the UV light transmitted to the photomultiplier. Emission fluorescence was detected using an external fast microchannel plate photomultiplier tube (Hamamatsu R3809U-50) and recorded using a time-correlated single photon counting (TCSPC) PC module SPC830 (Becker and Hickl GmbH, Berlin, Germany). Fluorescence lifetime image microscopy was performed by synchronizing the XY galvanometer positions with the fluorescence decay.

Neutron and X-ray Reflection Measurements. Reflection of neutrons and X-rays occurs where there is an interface between two materials with different refractive indices for the respective probe. The refractive index of a material to X-rays is related to the number of electrons in the component atoms, whereas for neutrons, the refractive index depends upon the nuclear properties of the particular isotopes present. The reflected beam can be used to determine properties such as the amount and thickness of the layer of material giving rise to the reflection, as explained later. Further details of the use of X-ray and neutron reflections to study monolayers at the air−water interface can be found in recent reviews.[42−44]

The reflectivity experiments described here were performed by adding a monolayer film of either pure peptide or a peptide/lipid mixture to an aqueous subphase. The monolayer was compressed until the desired surface pressure was obtained;

DOI: 10.1021/acs.biochem.5b00308
Biochemistry 2015, 54, 5185−5197

then the area of the monolayer was held fixed, and the surface pressure and reflectivity to neutrons or X-rays were monitored continuously, first under a flow of pure oxygen and then under a dilute flow of ozone in oxygen. The neutron reflectivity experiments with the pure peptide monolayers were performed on the FIGARO reflectometer at the Institut Laue-Langevin (Grenoble, France), whereas the experiments involving the anionic lipids POPG and DPPG were performed on the SURF reflectometer at ISIS, Rutherford Appleton Laboratory (Harwell Oxford, U.K.).[45,46] The neutrons entered and exited the environmental chamber via fused quartz windows. For experiments performed above room temperature, the windows were heated to prevent the condensation of water vapor. The reflection of visible laser light at the interface was used to check regularly the height alignment of the interface with respect to the neutron beam. The incident neutron beam with a range of wavelengths, λ (2.2−25 Å for FIGARO and 0.5−6.5 Å for SURF), was collimated and inclined so that it fell at a grazing angle of incidence, θ, of either 0.624° and 3.78° (FIGARO) or 1.5° (SURF) to the horizontal plane of the air−liquid interface. This provided neutron reflectivity data as a function of momentum transfer normal to the interface, q, where $q = (4\pi/\lambda) \sin \theta$. The measured reflectivity of a sample of pure D_2O contained in the Langmuir trough was used to obtain a scale factor with which to normalize the intensity spectrum of the incident beam.

The X-ray reflectivity experiments were performed on beamline I07 at Diamond Light Source.[47] The X-rays had a wavelength, λ, of ∼1.0 Å (12.5 keV), entered the chamber via a mica window, and exited the chamber via a Kapton window. A Pilatus area detector was used with regions of interest defined for the reflected beam and the background. The incident X-ray beam on I07 can be deflected to fall at a range of angles of incidence to the air−liquid interface, allowing the reflectivity to be measured as a function of q. In this work, the reflectivity was recorded between q values of 0.015 $Å^{-1}$, below the critical edge where total reflection occurs, and 0.8 $Å^{-1}$. Beam damage to the sample was avoided by the use of a fast shutter that blocked the beam from reaching the sample at all times other than when measurements were actually being made and by regularly moving the beam footprint roughly 1 mm so that different portions of the monolayer were being sampled over the course of an experiment (several hours). Tests revealed that when using this procedure no noticeable difference in the reflectivity was evident after several hours for a film exposed to only a continuous flow of oxygen.

The reflectivity of an interface for X-rays depends upon the X-ray scattering-length density of the material at the interface, the thickness of the interfacial material, and, to a smaller extent, the wavelength of the X-rays when near an absorption edge. The X-ray scattering-length density of a molecule, ρ_e, is given by

$$\rho_e = \frac{\sum_i Z_i r_e}{V} \quad \text{(I)}$$

where Z_i values are the atomic numbers of the individual nuclei in the molecule (the sum is over all nuclei in the molecule), r_e is the classical radius of an electron, and V is the volume occupied by one molecule. The scattering-length density of any material for X-rays is therefore positive and increases with increasing electron density. The values of $\sum_i Z_i r_e$ for the molecules considered in this work are listed in Table 1. The benefits of isotopic substitution, so useful in neutron reflectometry, as explained below, are not available as part of X-ray reflectometry; however, X-ray sources are significantly more intense than neutron source, and the technique gives lower background scattering, thus allowing much lower values of reflectivity to be accurately determined.

Table 1. Formulae, Values of $\sum_i Z_i r_e$ and $\sum_i b_{n,i}$ for the Compounds Used in the X-ray and Neutron Reflection Experiments[a]

compound	formula	$\sum_i Z_i r_e$ (fm)	$\sum_i b_{n,i}$ (fm)
SP-$B_{(1-25)}$	$C_{139}N_{35}O_{28}S_3H_{223}$	4444	588
SMB	$C_{217}N_{61}O_{46}S_6H_{363}$	7217	938
[^{1}H]DPPC	$C_{40}H_{80}NO_8P$	1146	28
d_{62}-DPPC	$C_{40}H_{18}D_{62}NO_8P$	1146	673
d_{31}-POPG	$C_{40}H_{45}D_{31}O_{10}PNa$	1192	371
[^{1}H]POPG	$C_{40}H_{76}O_{10}PNa$	1192	48
d_{62}-DPPG	$C_{38}H_{12}D_{62}O_{10}PNa$	1152	688
[^{1}H]DPPG	$C_{38}H_{74}O_{10}PNa$	1152	42

[a]The sum is over the all the nuclei in the molecule.

The reflectivity of an interface for neutrons depends upon the neutron scattering-length density and the thickness of the interfacial material. The neutron scattering-length density, ρ_n, of a molecule is given by eq II:

$$\rho_n = \frac{\sum_i b_{n,i}}{V} \quad \text{(II)}$$

where $b_{n,i}$ values are the coherent neutron scattering lengths of the individual nuclei in the molecule, a property that is sensitive to the nuclear composition (the sum is again over all nuclei in the molecule), and V is again the volume occupied by one molecule. As the coherent scattering lengths of hydrogen (−3.74 fm) and deuterium (6.67 fm) are of opposite sign, a solution of null reflecting buffered water (NRW) can be made with a mixture of H_2O and D_2O that has a scattering length for the mixture, $\sum_i b_{n,i}$, where the sum over all atoms in the mixture is zero and consequently the scattering-length density, ρ_n, of the mixture is zero. When a monolayer of material is present on a NRW subphase, specular reflection of neutrons occurs from the monolayer material only, and the product of the neutron scattering-length density and the thickness of the observed layer relates directly to the amount of material at the interface.[44] A reduction in reflectivity from a monolayer spread on NRW following reaction can be directly related to a loss of material from the interface, e.g., through solubilization and/or volatilization of material. In the case of neutrons, the difference in sign of the scattering lengths of H and D means that the use of different deuteration schemes can dramatically change the scattering length of different isotopologues. The scattering lengths, $\sum_i b_{n,i}$, of the various molecules used in neutron reflection experiments in this work are listed in Table 1. Peptides SP-B(1−25) and SMB both contain exchangeable hydrogen atoms. When the peptides were on a D_2O subphase, 47 hydrogens were expected to exchange for deuteriums in the case of SP-B(1−25) and 81 in the case of SMB. When the peptides were on NRW buffer, only 8% of these exchangeable hydrogen atoms would be expected to be replaced by deuterium atoms.

DOI: 10.1021/acs.biochem.5b00308
Biochemistry 2015, 54, 5185−5197

RESULTS

Exposure to gas-phase ozone of monolayers of SP-$B_{(1-25)}$, SMB, and mixed monolayers containing the peptides and lipids leads to a rapid reaction of the monolayer, as revealed by surface pressure measurements. Figure 2 shows the change in surface pressure when a monolayer of SP-$B_{(1-25)}$ and a monolayer of SMB, at 37 °C, is exposed to ∼1 ppm of gas-phase ozone.

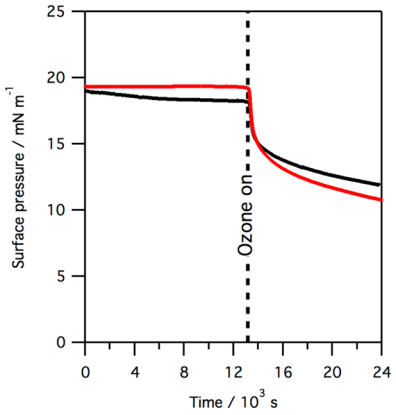

Figure 2. Plot of surface pressure vs time when a monolayer of pure SP-$B_{(1-25)}$ (black line) or SMB (red line) is exposed to ∼1 ppm gas-phase ozone. Data were recorded at 37 °C.

As shown in Figure 2, exposure to ozone causes a sharp drop in surface pressure, corresponding to a rise in surface tension, when monolayers of either SP-$B_{(1-25)}$ or SMB are exposed to gas-phase ozone. The drop is more pronounced in the case of SMB. The rapid drop in surface pressure is followed by a much slower decline in surface pressure over many hours. Exposure to ozone of monolayers of SP-$B_{(1-25)}$ and DPPC, or SMB and DPPC, also leads to a rapid drop in surface pressure, but the absolute reduction in surface pressure is less pronounced. An example is shown in Figure 3 for the reaction of a 1:1 by weight (∼1:6 by molecule) monolayer of SMB and DPPC. We have previously shown that exposure of monolayers of pure DPPC to parts per million levels of ozone does not lead to a change in the surface pressure.[22]

The positively charged protein SP-B is thought to be closely associated with the negatively charged unsaturated lipid POPG in lung surfactant. We have previously shown that the related unsaturated lipid POPC reacts readily with ozone to give an initial rise in surface pressure, followed by a slow fall.[22,23] Neutron reflection studies with POPC revealed that exposure to ozone led to a rapid loss of the terminal C9 portion of the oleoyl chain from the interface and that this loss was accompanied by an increase in surface pressure. It was therefore suggested that the portion of the oxidized oleoyl tail still attached to the lipid headgroup underwent a change in orientation and penetrated the air−water interface, thus increasing the surface pressure, a suggestion supported by molecular dynamics simulations.[23,48] In the work presented here, the reaction of a monolayer of POPG with gas-phase ozone was found to be similar to that of POPC. Figure 4 shows the changes in surface pressure observed when a monolayer of POPG with an initial surface pressure of ∼20 mN m^{-1} is exposed to ozone.

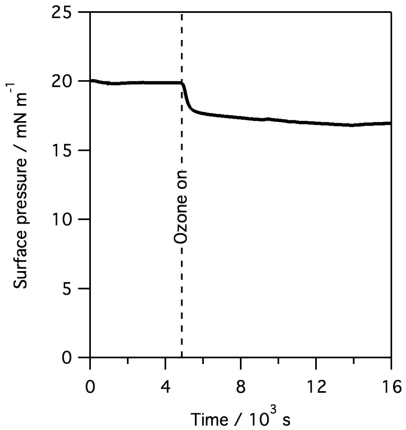

Figure 3. Plot of surface pressure vs time when a monolayer of SMB and DPPC, 1:6 by molecule, is exposed to ∼1 ppm gas-phase ozone. Data were recorded at 36 °C.

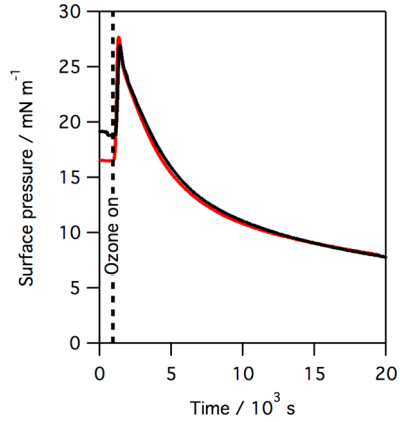

Figure 4. Plot of surface pressure vs time when a monolayer of POPG (red line) and a monolayer of SMB and POPG, 1:12 by molecule (black line), is exposed to ∼2 ppm gas-phase ozone.

As shown in Figure 4, exposure of a monolayer of POPG to ozone causes a change in surface pressure much more dramatic than that observed for monolayers of either SP-$B_{(1-25)}$ or SMB (Figure 2). When a mixed monolayer of SMB and POPG (1:12 by molecule) at the air−water interface is exposed to ozone, a significant increase in surface pressure is again seen, as shown by the black line in Figure 4, followed by a steady, slow drop in the surface pressure. In contrast to POPG, when the saturated anionic lipid DPPG is exposed to ozone no change in surface pressure is observed, as was previously reported for monolayers of the saturated zwitterionic lipid DPPC, indicating that in the case of both DPPG and DPPC no reaction with ozone has occurred. The change in surface pressure when a monolayer of SMB and DPPG, 1:12 by molecule, is exposed to ozone is shown in Figure 5.

As can been seen, when SMB is present with DPPG, there is only a slight decrease in the surface pressure when the monolayer is exposed to ozone, compared to the case in which the monolayer is SMB only (Figure 2) or SMB and DPPC (Figure 3), suggesting the anionic lipid DPPG might be protecting the SMB to a greater extent than the zwitterionic DPPC lipid. It should be remembered that DPPG is not present in significant quantities in the lung, where the dominant PG lipids are all unsaturated.

In summary, exposure of monolayers of either of the two peptide mimics of SP-B, SP-$B_{(1-25)}$, or SMB to ozone causes a

DOI: 10.1021/acs.biochem.5b00308
Biochemistry 2015, 54, 5185−5197

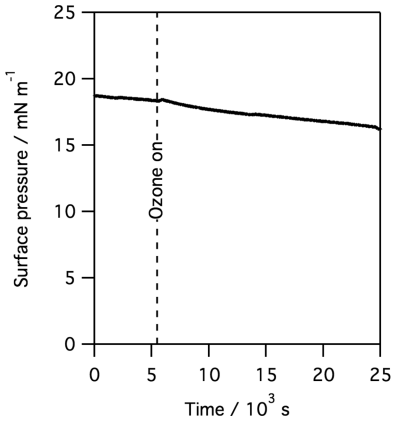

Figure 5. Plot of surface pressure vs time when a monolayer of SMB and [^{2}H]DPPG, 1:12 by molecule, is exposed to ∼2 ppm gas-phase ozone. Data were recorded at room temperature.

rapid drop in the surface pressure. If the peptides are present in monolayers with lipids, then changes in surface pressure suggest both reaction of the peptide and, if the lipid is unsaturated, reaction of the lipid may occur.

A number of residues in SP-B$_{(1-25)}$ and SMB can potentially react with gas-phase ozone, when the peptide is spread at the air−water interface, depending upon the positioning of the peptide at the interface.[49] The fluorescence of the only tryptophan residue in SMB, Trp9, gives a strong fluorescence signal at the interface, as shown in Figure 6. The fluorescence

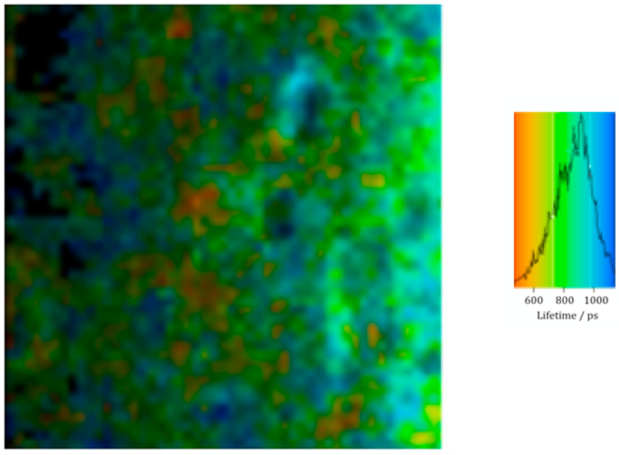

Figure 6. Fluorescence lifetime image microscopy of a monolayer of SMB at the air−water interface recorded using two-photon excitation at 590 nm and monitoring the fluorescence at 380 nm. The color scale shown on the right is for the mean excited state lifetime. After exposure for 600 s to ∼3 ppm ozone in air, no fluorescence was detected.

intensity alone of a molecule is insufficient to determine the environment of the molecule under observation so that the determination of the excited state lifetime provides an advantage. In the case of fluorescence from tryptophan in SMB at the air−water interface, the observed excited state lifetime has two components, 0.6 and 2.5 ns (weighted average of 0.9 ns), both shorter than the 2.8 ns lifetime generally observed for tryptophan, indicating that the tryptophan in SMB at the air−water interface is in a complex environment. Exposure to ∼3 ppm ozone gas resulted in a rapid decrease in fluorescence intensity and prevented a detailed study of the changes in fluorescence lifetime with exposure to be made in this work. After exposure to ∼3 ppm ozone for 10 min, no discernible fluorescence could be detected from the sample using the same excitation and emissions wavelengths. We can conclude that the tryptophan residue in SP-B reacts rapidly with ozone on a time scale comparable to that of the reaction that causes the rapid decrease in surface pressure.

Both X-ray and neutron reflection measurements were taken to examine the amount and thickness of peptide monolayers at the air−water interface following exposure to gas-phase ozone of monolayers of SP-B$_{(1-25)}$ and SMB on a buffered aqueous subphase. The surface pressure was recorded during these X-ray and neutron reflectometry experiments. Figure 7 shows

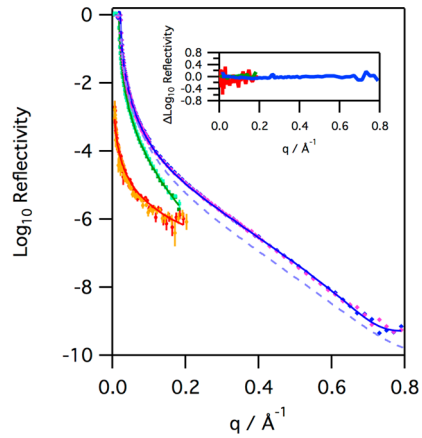

Figure 7. Reflectivity profiles for monolayers of SP-B$_{(1-25)}$, with an initial surface pressure of 18 mN m^{-1}, on H_2O buffer (diamonds, blue before ozone, pink after, X-ray data recorded at 21 °C), D_2O buffer (squares, dark green before ozone, light green after, neutron data recorded at 32 °C), and NRW buffer (circles, red before ozone, orange after, neutron data recorded at 37 °C) before and after exposure to ozone for 20400 s at ∼2 ppm (X-ray data), 9072 s at ∼1 ppm (neutron data with NRW), and 5769 s at ∼1 ppm (neutron data with D_2O). The solid lines represent the fits to the data before ozone, as described in the text. The dash light blue line represents the reflectivity to X-rays of a clean aqueous buffer interface for reference. The inset shows the change in the reflectivity before and after ozone, specifically the difference between the logarithms of the reflectivity recorded before and after ozone exposure.

reflectivity data obtained for SP-B$_{(1-25)}$ on buffer before and after exposure to ozone. Three scattering contrasts are shown: that from X-rays and those from neutrons involving two isotopic contrasts of the subphase (NRW and D_2O). In the case of X-rays, the presence of the peptide at the air−water interface significantly changes the reflectivity profile from that recorded for just the buffer alone. In the case of neutrons, the weak reflectivity comes from the presence of the peptide at the interface when spread on a NRW buffer, and the strong reflectivity of the subphase is modified by the presence of the peptide at the interface when spread on a D_2O buffer.

The reflectivity data recorded before and after ozone are almost identical, with any differences appearing to be just random error (see the inset in Figure 7), at least within the sensitivity of the instruments used. The three reflectivity profiles were fitted simultaneously to determine the characteristics of the peptide at the interface. The peptide film can be modeled as two layers with part immersed in the aqueous subphase and the top layer in air (see the Supporting

DOI: 10.1021/acs.biochem.5b00308
Biochemistry 2015, 54, 5185−5197

Information for further details). The fits obtained, which are shown in Figure 7, show that most of the SP-$B_{(1-25)}$, 88 ± 5%, lies above the water in a layer approximately 8 Å thick, with a highly hydrated thinner layer, ~6 Å, that lies in the aqueous subphase containing the remainder of the peptide. The thickness of the hydrated layer and the fact that it contains only a small amount of the peptide material are qualitatively consistent with a model of the peptide as an α-helix on the surface of the subphase with just the hydrophilic arginine and lysine side chains extending into the subphase as a hydrated layer. In all three cases, the reflectivity appears to be unchanged, within experimental error, after prolonged exposure to ozone gas. Thus, although the surface pressure data clearly show that the peptide reacts with ozone, the reflectivity data reveal that the oxidized material remains at the air−water interface, and there is no evidence of deeper penetration into the aqueous subphase upon prolonged exposure to ozone.

The reaction of SMB with ozone also produced very little change in the X-ray and neutron reflectivity profiles of the interface, with any differences in the reflectivity before and after ozone appearing to be just random error, as shown in Figure 8.

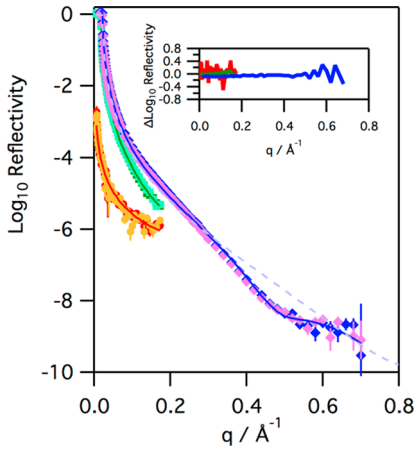

Figure 8. Reflectivity profiles for monolayers of SMB on H_2O buffer (diamonds, blue before ozone, pink after, X-ray data recorded at 21 °C, initial surface pressure of 20 mN m^{-1}), D_2O buffer (squares, dark green before ozone, light green after, neutron data recorded at 38 °C, initial surface pressure of 15 mN m^{-1}), and NRW buffer (circles, red before ozone, orange after, neutron data recorded at 37 °C, initial surface pressure of 19 mN m^{-1}) before and after exposure to ozone for 9900 s at ~2 ppm (X-ray), 29600 s at ~1 ppm (neutron NRW data), and 30900 s at ~1 ppm (neutron D_2O data). The solid lines, dashed blue line, and inset are described in the legend of Figure 7.

Simultaneous fitting of the combined X-ray and neutron reflection data for SMB in the same way as described for SP-$B_{(1-25)}$ reveals that the SMB is positioned at the interface with 70 ± 7% in a layer of thickness 7 Å above the water and the remaining fraction in a hydrated 7 Å layer in the subphase. As can be seen from Figure 8, the reaction of monolayers of SMB at the air−water interface does not lead to any significant change in the neutron or X-ray reflectivity profiles, whether the reaction was performed at 21 °C or the more physiologically relevant temperature of 37 °C. Fitting the data recorded after exposure of SMB to ozone reveals no changes, outside the uncertainty, in the amount of material at the interface or the positioning of the peptide at the interface. This is a surprising result as the fluorescence data clearly show that the tryptophan residue of SMB is quickly oxidized by ozone under these conditions and the reaction leads to a significant change in the surface pressure.

The nature of the reaction products that remain at the interface was investigated by performing SDS−PAGE and HPLC analysis of the reaction mixture extracted from the interface with chloroform, as described above. Figure 9 shows a

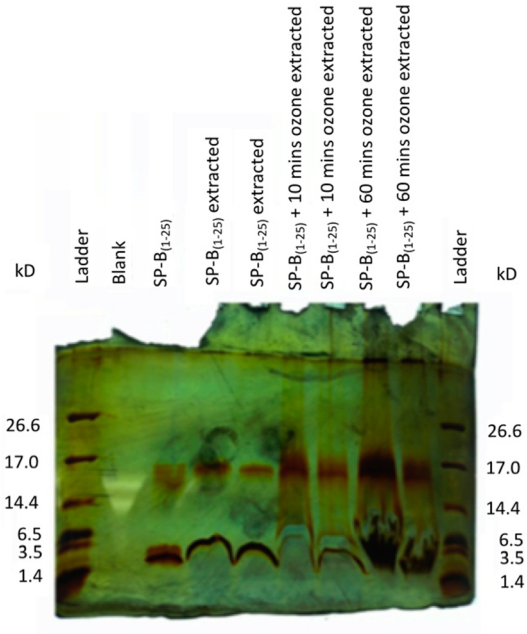

Figure 9. SDS−PAGE gel showing SP-$B_{(1-25)}$ recovered from the air−water interface subject to oxygen only, and after exposure to ~3 ppm ozone gas for 10 and 60 min.

polyacrylamide gel of the extracted material from a monolayer of SP-$B_{(1-25)}$ that has not been exposed to ozone and also material that has been exposed to ozone. The gel reveals that after oxidation with ozone (~3 ppm for 600 and 3600 s), the peptide still shows a band in the same place in the gel; i.e., no significant fragmentation of the peptide chain has occurred as short products are not seen in the gel. Streaking is evident in the gel for the samples that have been exposed to ozone, and the extent of streaking increases with increasing exposure time. The streaking reveals that, unlike the initial peptide, the oxidized peptide recovered is not fully soluble in the SDS−PAGE aqueous running buffer used.

The band for SP-$B_{(1-25)}$ (mass of 2.9 kDa) can be seen on the gel, as can a band for an oligomer of SP-$B_{(1-25)}$. The assignment of this band as an oligomer is confirmed by its absence when a sample of SP-$B_{(1-25)}$ is heated with the reductant DTT before being loaded into the gel (see Figure S2). In a different series of experiments, the material recovered from the interface was collected and concentrated in chloroform and then analyzed by HPLC. The results are shown in Figure 10.

The results shown in Figure 10 reinforce the results obtained from the SDS−PAGE experiment, that reaction of SP-$B_{(1-25)}$ with ozone does not lead to the formation of any small hydrophilic fragments, and the peptide itself is rendered more hydrophobic upon oxidation, presumably via some structural change and/or formation of higher-order oligomers.

In a similar series of experiments, monolayers of SMB at the air−water interface were exposed to gas-phase ozone and the oxidized material was collected using chloroform as described

DOI: 10.1021/acs.biochem.5b00308
Biochemistry 2015, 54, 5185−5197

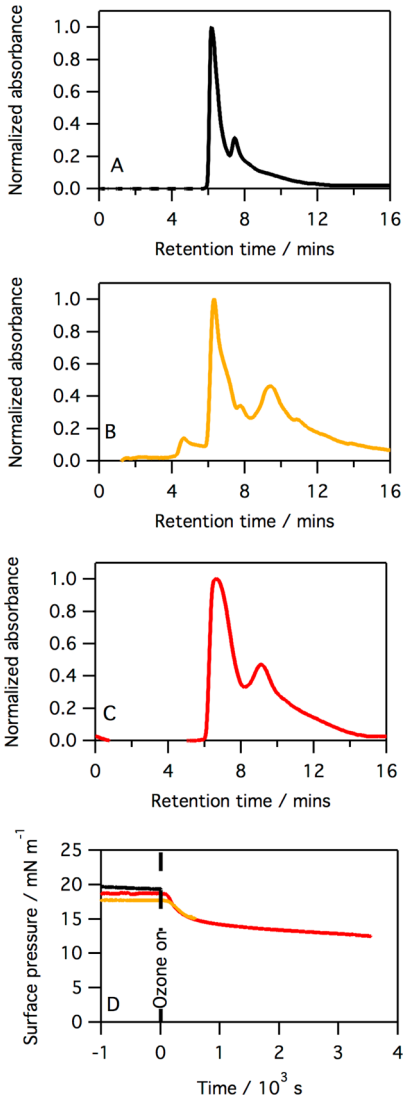

Figure 10. Chromatogram of material extracted into chloroform for monolayers on an aqueous buffered subphase of SP-$B_{(1-25)}$ (A), SP-$B_{(1-25)}$ after exposure to ozone for 10 min (B), and SP-$B_{(1-25)}$ after exposure to ozone for 60 min (C). All peaks have been background subtracted and normalized to the absorption, at 254 nm, of the SP-$B_{(1-25)}$ peak at ~6.5 min. Panel D shows the surface pressure vs time for the monolayer immediately before extraction with chloroform: no ozone (black line), after exposure to ozone for 10 min (orange line), and after exposure to ozone for 60 min (red line).

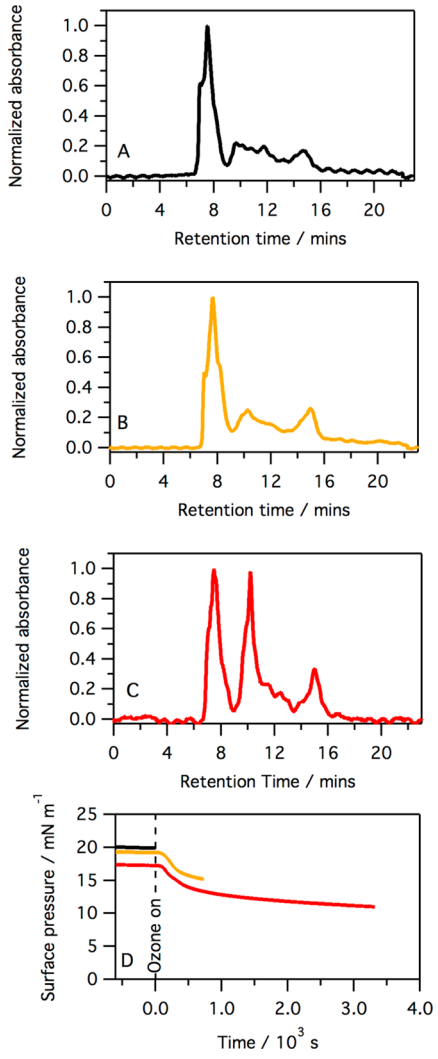

Figure 11. HPLC data equivalent to those shown in the previous figure but for SMB (see the legend of Figure 10 for details). The normalization was conducted using the peak at ~7.5 min.

previously. Figure 11 shows the chromatograms obtained when a monolayer of SMB was extracted after exposure to oxygen only, after exposure to ~3 ppm ozone for 10 min, and after exposure to ~3 ppm ozone for 60 min. The absolute efficiency of the extraction/recovery procedure is variable, so the peaks have been normalized to the intensity of the SMB peak.

Following exposure to ozone for 10 min, the surface pressure of a monolayer of SMB has already dropped sharply (see Figure 2); however, as shown in Figure 11, no new peak is observed in the chromatograms, indicating that the product of the initial reaction co-elutes with the starting material. After exposure to ozone for 60 min, the intensity of a peak with a retention time of ~15 min, a retention time longer than that for SMB, has significantly increased compared to that of the SMB peak. This implies that a reaction product is formed slowly and, as it is eluted after SMB under the reverse-phase chromatographic conditions employed, this slow-forming product must be more hydrophobic than the starting material SMB.

The experiments described so far reveal that both SP-$B_{(1-25)}$ and SMB are oxidized by low levels of ozone at the air−water interface, which causes a significant change in the surface pressure, yet the reaction products remain at the interface. A second set of reflectivity measurements were taken on mixed monolayers of SMB and anionic lipids to probe if oxidation of SMB changes its ability to interact with the anionic lipids. The unsaturated anionic lipid POPG has been shown to react with gas-phase ozone when present at the air−water interface (Figure 4). The reflectivity to neutrons of a monolayer of d_{31}-POPG on NRW decreases upon exposure to gas-phase ozone, as shown in Figure 12. As the subphase is NRW buffer, this reduction in reflectivity can be directly linked to the loss of material from the monolayer, and a reduction in the total value of the coherent neutron scattering length, b_n, for the monolayer, as shown in the inset in Figure 12. The neutron reflectivity data were fitted using a model of a single lipid layer on NRW, allowing the decrease in b_n for the monolayer with exposure time to ozone to be determined. This decrease in b_n followed the form of a single-exponential function shown in eq III:

DOI: 10.1021/acs.biochem.5b00308
Biochemistry 2015, 54, 5185−5197

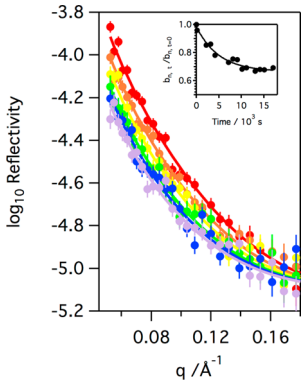

Figure 12. Neutron reflectivity profiles obtained at different exposure times when a monolayer of d_{31}-POPG on NRW at room temperature is exposed to ~3 ppm gas-phase ozone: $t = 0 \times 10^3$ s (red circles), $t = 2 \times 10^3$ s (orange circles), $t = 4 \times 10^3$ s (yellow circles), $t = 7 \times 10^3$ s (green circles), $t = 10 \times 10^3$ s (blue circles), and $t = 18 \times 10^3$ s (gray circles). The inset shows the relative decrease in the coherent neutron scattering length, b_n, for the monolayer material with time.

$$b_{n,t}/b_{n,t=0} = A + Be^{-Ct} \quad \text{(III)}$$

The fit to eq III, shown by the solid line in the inset in Figure 12, reveals that the b_n for the monolayer falls to 67 ± 2% of the initial value. As the b_n value for the monolayer is dominated by the contribution from the deuterated palmitoyl chain of d_{31}-POPG, this reduction in b_n is interpreted as a loss of deuterated material from the interface.

Exposure of a monolayer of SMB and d_{31}-POPG (1:12 by molecule) to ozone has been shown to lead to a rapid reaction (see Figure 4). The neutron reflectivity of this SMB and d_{31}-POPG monolayer on NRW is dominated by the d_{31}-POPG as d_{31}-POPG molecules contribute 83% of the total initial b_n value for the monolayer (81% of the overall scattering-length density). The neutron reflectivity for the SMB/d_{31}-POPG monolayer on NRW was therefore modeled as a single layer on NRW, similar to that of the pure lipid monolayer. Exposure of the monolayer to gas-phase ozone leads to a rapid drop in the reflectivity of the monolayer and the total b_n value for the monolayer, as shown in Figure 13.

Figure 13 shows that the reflectivity of the monolayer of SMB and d_{31}-POPG to neutrons decreases upon exposure of the monolayer to ozone gas and indicates that material is being lost from the monolayer and the total b value for the monolayer decreased upon exposure to ozone. Fitting the decrease in b for the monolayer to an exponential function (eq III) reveals that the final monolayer has a b value that is 62 ± 1% of the initial value for the monolayer. This is, surprisingly, slightly less than the value obtained when just d_{31}-POPG is present, without SMB, at the interface. A decrease in total b_n to ~73% of the initial value would be expected for the mixed monolayer if just material from d_{31}-POPG were lost from the interface (no loss of SMB) and the loss of material from POPG were not influenced by the presence of the SMB. It is not possible to determine, from the data recorded, whether the additional loss of material is due to the loss of more POPG from the interface when SMB is present or whether the presence of POPG causes some SMB to be lost from the interface upon oxidation. Further experiments in the future, with a deuterated version of SMB, would be required to answer this question. To examine selectively changes upon oxidation of SMB to interactions with the anionic headgroup of POPG, we also performed neutron

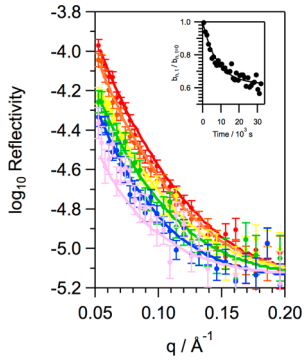

Figure 13. Neutron reflectivity profiles obtained at different exposure times when a monolayer SMB and d_{31}-POPG (1:12 by molecule) on NRW at room temperature is exposed to ~3 ppm gas-phase ozone: $t = 0$ s (red circles), $t = 2 \times 10^3$ s (orange circles), $t = 4 \times 10^3$ s (yellow circles), $t = 7 \times 10^3$ s (green circles), $t = 10 \times 10^3$ s (blue circles), and $t = 18 \times 10^3$ s (violet circles). The inset shows the relative decrease in the coherent neutron scattering length, b_n, for the monolayer material with time, and the solid line is obtained by fitting b_n to a single-exponential decay.

reflectivity studies in which mixtures of SMB and the saturated anionic lipid d_{62}-DPPG, 1:12 by molecule, on NRW buffer were exposed to ozone. The changes in surface pressure for this mixture are presented in Figure 5. There was no measurable reduction in the neutron reflectivity; thus, we can conclude that oxidation of SMB does not lead to a loss of d_{62}-DPPG from the interface (shown in Figure S3). X-ray reflectivity experiments (also Figure S3) revealed that when mixtures of SMB and DPPG (1:12 by molecule) on aqueous buffer were exposed to ozone for several hours the slight change in surface pressure was not accompanied by a significant change in the reflectivity of the interface. These data thus show that the small change in surface pressure when SMB/DPPG monolayers are exposed to ozone is not accompanied by significant loss of material from the interface or a measurable structural change.

DISCUSSION

The surface pressure results presented here for both peptide mimics of SP-B, SP-B$_{(1-25)}$ and SMB, clearly reveal that, at the relatively modest initial surface pressures considered in this work, exposure of the peptides to ozone at the air−water interface causes a rapid reaction leading to a reduction in surface pressure, corresponding to an increase in surface tension. As the peptides contain only residues found in full-length SP-B, we can conclude that SP-B will also react rapidly with ozone. At the air−water interface of the lung, SP-B will be surrounded by lipids. The most abundant lipid is DPPC. The surface pressure data show that both peptides also react with ozone when it is present with DPPC at the air−water interface. The reaction is less pronounced, but still occurs, when the anionic lipid DPPG is used in place of DPPC. The extent to which the presence of anionic lipids might offer some protection to SP-B in the lung is, however, uncertain as the anionic lipids found in the lung are not saturated lipids such as DPPG but rather unsaturated lipids such as POPG. As we have shown here, the unsaturated anionic lipid POPG itself reacts rapidly with ozone. This reaction may weaken the ability of POPG to hinder the reaction of ozone with SP-B. Kim et al.[24] have previously shown that both SP-B$_{(1-25)}$ and the neutral, unsaturated lipid, 1-palmitoyl-2-oleoyl-*sn*-glycerol (POG), react with ozone when both are present at the air−water interface.

DOI: 10.1021/acs.biochem.5b00308
Biochemistry 2015, 54, 5185−5197

Future studies of the reaction of ozone with monolayers of SP-B in the presence of the complex lipid mixtures found in natural lung surfactant are necessary to address this question. It would also be interesting to follow the extent of reaction of SP-B as a function of initial surface tension, as surface tensions present in the lung are lower than those studied here and the shielding of SP-B from the gas-phase ozone may be different.

As mentioned previously, Kim et al. found that SP-$B_{(1-25)}$ reacted with high levels of ozone when the peptide was at the air−water interface.[24] Tryptophan and methionine reacted, whereas cysteine residues did not. This is in contrast to the finding of Enami et al., who studied the reaction of free cysteine and ozone at the air−water interface and found that cysteine sulfenate, cysteine sulfinate, and cysteine sulfonate were all formed, whereas cystine was not.[50] In this work, the peptide SMB is shown to react with ozone at a rate very similar to that of SP-$B_{(1-25)}$. In SMB, unlike SP-$B_{(1-25)}$, all the initial cysteine residues have been converted into cystine, which is not thought to react with ozone.[50,51] Both SP-B(1−25) and SMB have one tryptophan residue; however, SMB has two methionine residues, whereas SP-$B_{(1-25)}$ has only one. The results from our fluorescence experiments clearly show that the rapid drop in surface pressure seen when SMB is exposed to ozone is accompanied by the rapid loss in fluorescence from tryptophan residues at the interface. The most likely reason for this is the tryptophan residues are oxidized rapidly when peptide SMB is exposed to ozone at the air−water interface. The slightly more pronounced drop in surface pressure when SMB is exposed to ozone compared to SP-$B_{(1-25)}$ can be attributed to a larger structural change upon oxidation of the tryptophan residues or the presence of an additional methionine residue that is oxidized in SMB compared to SP-$B_{(1-25)}$.

The results of our work are in agreement with those of Kim et al.[24] in that peptide SP-$B_{(1-25)}$ reacts rapidly with ozone at the air−water interface. In addition, we have shown the reaction occurs when ozone concentrations an order of magnitude lower than those used by Kim et al. are used. Our results do not support the suggestion by Kim et al. that the oxidation of SP-$B_{(1-25)}$ at the air−water interface by ozone leads to enhanced solubility of the peptide and deeper penetration into the aqueous layer. The neutron reflection experiments with NRW buffer and the X-ray reflection experiments on buffered water together clearly show that the oxidized peptide remains at the interface and is not solubilized, and that there are no measurable structural changes in the monolayer. The neutron reflection experiments using a buffered D_2O subphase are specifically sensitive to the degree of penetration of the peptide into the aqueous layer, and oxidation is seen to make no measurable change in this degree of penetration (see Figure 7). This result requires some thought as the oxidation of tryptophan by ozone to *N*′-formylkynurenine (see Scheme 1) and the oxidation of methionine to methionine sulfoxide do increase the hydrophilicity of these two residues (oxidation of the cysteine residues would also increase the hydrophilicity if it is occurring). The tryptophan, residue 9 of the peptide, and the methionine, residue 21, are positioned at either end of the α-helical region of SP-$B_{(1-25)}$. Sarker et al. have previously shown that replacement of tryptophan in SP-$B_{(8-25)}$ with the oxidized form, kynurenine (see Scheme 1), leads to a loss of helical character and a change in the interaction of the peptide with lipids.[52] It would be reasonable to assume that oxidation of tryptophan to *N*-formylkynrenine would also lead to a loss of helical character.

Scheme 1. Formation of an *N*′-Formylkynurenine Residue from a Tryptophan Residue[a]

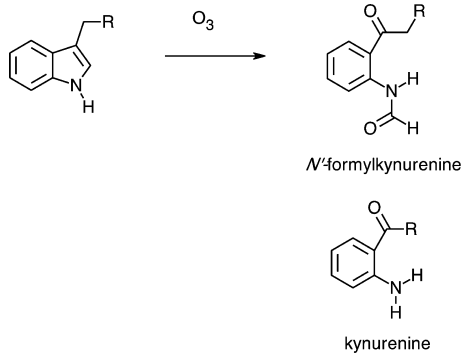

[a]The structure of kynurenine is shown below.

There are many examples in the literature to show that oxidation of methionine to methionine sulfoxide leads to changes in protein structure and stability (e.g., ref 53). A reduction in the level of secondary structure of the peptides is consistent with the results from our reverse-phase HPLC experiments. The material extracted after oxidation shows that there is slow formation of a product material with a longer retention time and, hence, a substance more hydrophobic than the starting material. The formation of the more hydrophobic substance is much slower than the initial oxidation of the tryptophan residue, in keeping with the idea that the peptide containing the oxidized tryptophan, possibly methionine, residue undergoes a slow conformational change. The SDS−PAGE results reveal that peptide SP-$B_{(1-25)}$ is not cleaved following exposure to ozone; rather, ozone exposure leads to more oligomerization of the peptide, and the streaking observed in the gel for the oxidized sample is consistent with the peptide being less soluble in aqueous media following oxidation. Thus, in the case of SP-$B_{(1-25)}$, we see that the peptide reacts rapidly with low levels of ozone at the air−water interface and the oxidation does not lead to solubilization of the peptide from the interface. On the other hand, the oxidized material remains at the interface and undergoes substantial conformational changes, leading to a more hydrophobic product and an increased level of oligomerization. The X-ray and neutron reflectivity data show no significant differences after exposure to ozone; that is, the fraction of the peptide in the hydrophobic layer above the water and the fraction in the hydrated aqueous layer does not change upon oxidation within the precision of the measurements. This behavior is in keeping with our earlier suggestion that the peptide material in the hydrated layer is essentially just the hydrophilic arginine and lysine chains that are unchanged by oxidation. The rearrangement of the protein occurs in the already hydrophobic layer in the air, which becomes more hydrophobic upon exposure to ozone. In the case of exposure of SMB to ozone, again the slow growth of a peak in the HPLC analysis at a longer retention time to the initial material is consistent with a major conformational change in the peptide following ozone oxidation. It should be noted that the results presented here show that no cleavage of the peptide chain has occurred upon exposure to ozone, which is similar to what has previously been shown when other soluble proteins are exposed to ozone in aqueous solutions.[54]

In addition to studies of the pure peptides at the air−water interface, we have also undertaken studies of the peptides when

DOI: 10.1021/acs.biochem.5b00308
Biochemistry 2015, 54, 5185−5197

they are present in lipid monolayers. The surface pressure measurements show that the main lung lipids do not shield the peptides from the ozone gas. A rapid drop in surface pressure occurs when both SMB and SP-$B_{(1-25)}$ in monolayers of the lipid DPPC are exposed to ozone. The lipid DPPC does not react with ozone. When SMB is present in monolayers with the unsaturated anionic lipid POPG, a rapid reaction of the lipid is clearly observed, and more material is lost from the interface than if just the lipid POPG were present. However, it is not possible to determine if the additional material lost is of lipid or peptide origin. The role of protein SP-B is thought to be to interact with unsaturated anionic lipids such as POPG, possibly by binding to the lipids and bringing them back to the interface as the lungs expand. The interaction is thought to be facilitated by the presence of several positively charged residues in SP-B. Looking at the experimentally determined structure of Mini-B, SP-B(8−25,63−78), PDB entry 1SSZ, shown in Figure 14, it

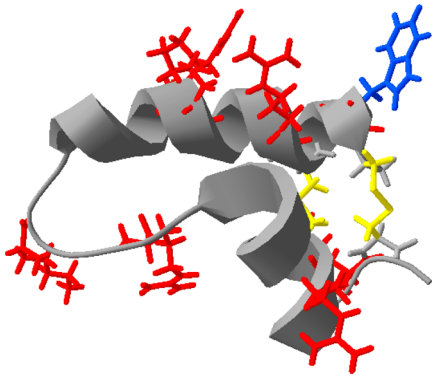

Figure 14. Structure of SP-$B_{(8-25,63-78)}$, known as Mini-B, PDB entry 1SSZ. The tryptophan residue is colored blue, and all positively charged amino acids, thought to interact with negatively charged phosphoglycerol lipids, are colored red. The disulfide bonds between the cysteine residues are colored yellow. Oxidation of the tryptophan is suggested to lead to local unwinding of the helical structure close to at least one of the arginine residues, potentially interfering with lipid binding.

can be seen that the positively charged arginine residue (residue 8 of Mini-B) is very close to the tryptophan, residue 2 of Mini-B. Oxidation of the tryptophan residue by ozone at the air−water interface has been shown in this work to occur and lead to a conformational change in the peptide, likely to include partial unwinding of the α-helix. Considering the structure shown in Figure 14, it is reasonable to conclude that this change in conformation is likely to affect the binding of anionic lipids to the arginine nearby. In future work, we will go on to look further at the interaction of oxidized SP-B with anionic lipids.

CONCLUSIONS

In this work, we have shown that two peptide mimics of the lung surfactant protein B, SP-B, react rapidly with low levels of the environmental pollutant gas-phase ozone when they are present at the air−water interface. The rapid reaction is evident from a change in the surface tension of the interface and loss of tryptophan fluorescence. The presence of lipids does not appear to shield the peptides from the ozone gas. The rapid oxidation of the peptides is followed by a slow conformational change leading to a product that is more hydrophobic than the starting material. The oxidized peptides remain at the interface after the reaction, but examination of the interfacial structures suggests that interaction with anionic lipids will be impaired. As full-length protein SP-B also contains the same residues as the peptide mimics studied here, we can conclude that inhalation of ozone will lead to oxidation of vital lung protein SP-B, leaving a damaged protein at the interface.

ASSOCIATED CONTENT

Supporting Information

The Supporting Information is available free of charge on the ACS Publications website at DOI: 10.1021/acs.biochem.5b00308.

As an example is shown the fit obtained to the X-ray data for SMB when a single-layer model is used, rather than a two-layer module for the peptide. An image of a polyacryalmide gel for a sample of SP-$B_{(1-25)}$ and a sample of SP-$B_{(1-25)}$ after heating with DTT is shown, confirming the band at ∼16 kDa is from an oligomer of SP-$B_{(1-25)}$. The X-ray and neutron reflectivity curves for monolayers of SMB and DPPG before and after ozone exposure are included (PDF)

AUTHOR INFORMATION

Corresponding Author

*E-mail: k.thompson@bbk.ac.uk.

Funding

J.M.H. thanks the Wellcome Trust for the provision of Studentship 093468/Z/10/Z. We acknowledge the ISIS Neutron Facility and Institut Laue-Langevin for access to neutron beam time on FIGARO and SURF and Diamond Light Source for time on beamline I07 under Proposal SI7258 that contributed to the results presented here.

Notes

The authors declare no competing financial interest.

ACKNOWLEDGMENTS

We thank Simon Wood, Institut Laue-Langevin, for technical support on FIGARO.

ABBREVIATIONS

DPPC, 1,2-dipalmitoyl-*sn*-glycero-3-phosphocholine; DPPG, 1,2-dipalmitoyl-*sn*-glycero-3-phosphoglycerol; DTT, dithiothreitol; HPLC, high-performance liquid chromatography; POPC, 1-palmitoyl-2-oleoyl-*sn*-glycero-3-phosphocholine; POPG, 1-palmitoyl-2-oleoyl-*sn*-glycero-3-phosphoglycerol; PAGE, polyacrylamide gel electrophoresis; NRW, null reflecting buffered water; SDS, sodium dodecyl sulfate; SP-B, surfactant protein B; SMB, Super Mini-B; Tris, tris(hydroxymethyl)aminomethane.

REFERENCES

(1) Creuwels, L. A., van Golde, L. M., and Haagsman, H. P. (1997) The pulmonary surfactant system: biochemical and clinical aspects. *Lung 175*, 1−39.

(2) Pérez-Gil, J. (2008) Structure of pulmonary surfactant membranes and films: The role of proteins and lipid−protein interactions. *Biochim. Biophys. Acta, Biomembr. 1778*, 1676−1695.

(3) Veldhuizen, R., Nag, K., Orgeig, S., and Possmayer, F. (1998) The role of lipids in pulmonary surfactant. *Biochim. Biophys. Acta, Mol. Basis Dis. 1408*, 90−108.

(4) Robillard, E., Alarie, Y., Dagenais-Perusse, P., Baril, E., and Guilbeault, A. (1964) Microaerosol administration of synthetic beta-

DOI: 10.1021/acs.biochem.5b00308
Biochemistry 2015, 54, 5185−5197

gamma-dipalmitoyl-l-alpha-lecithin in the respiratory distress syndrome: a preliminary report. *Can. Med. Assoc. J. 90*, 55−57.
(5) Chu, J., Clements, J. A., Cotton, E. K., Klaus, M. H., Sweet, A. Y., and Tooley, W. H. (1967) Neonatal pulmonary ischemia Part I: Clinical and physiological studies. *Pediatrics 40*, 709−782.
(6) Fujiwara, T., Maeta, H., Chida, S., Morita, T., Watabe, Y., and Abe, T. (1980) Artificial surfactant therapy in hyaline-membrane disease. *Lancet 315*, 55−59.
(7) Engle, W. A. (2008) Surfactant-replacement therapy for respiratory distress in the preterm and term neonate. *Pediatrics 121*, 419−432.
(8) Nogee, L. M., de Mello, D. E., Dehner, L. P., and Colten, H. R. (1993) Brief report: Deficiency of pulmonary surfactant protein B in congenital alveolar proteinosis. *N. Engl. J. Med. 328*, 406−410.
(9) Nogee, L. M., Garnier, G., Dietz, H. C., Singer, L., Murphy, A. M., de Mello, D. E., and Colten, H. R. (1994) A mutation in the surfactant protein B gene responsible for fatal neonatal respiratory disease in multiple kindreds. *J. Clin. Invest. 93*, 1860−1863.
(10) Verhasselt-Crinquette, M., Franquet-Ansart, H., Rakza, T., Storme, L., Copin, M. C., and Devisme, L. (2009) Congenital pulmonary alveolar proteinosis related to a surfactant protein B deficiency: report of two cases. *Ann. Pathol. 29*, 481−484.
(11) Tredano, M., Cneude, F., Denamur, E., Truffert, P., Capron, F., Manouvrier, S., Feldmann, D., Couderc, R., Elion, J., and Lacaze-Masmonteil, T. (2000) Constitutional deficiency of pulmonary surfactant protein B: clinical presentation, histologic and molecular diagnosis. *Arch. Pédiatrie 7*, 641−644.
(12) Clark, J. C., Wert, S. E., Bachurski, C. J., Stahlman, M. T., Stripp, B. R., Weaver, T. E., and Whitsett, J. A. (1995) Targeted disruption of the surfactant protein B gene disrupts surfactant homeostasis, causing respiratory failure in newborn mice. *Proc. Natl. Acad. Sci. U. S. A. 92*, 7794−7798.
(13) Glasser, S. W., Burhans, M. S., Korfhagen, T. R., Na, C.-L., Sly, P. D., Ross, G. F., Ikegami, M., and Whitsett, J. A. (2001) Altered stability of pulmonary surfactant in SP-C-deficient mice. *Proc. Natl. Acad. Sci. U. S. A. 98*, 6366−6371.
(14) Anderson, H. R., Spix, C., Medina, S., Schouten, J. P., Castellsague, J., Rossi, G., Zmirou, D., Touloumi, G., Wojtyniak, B., Ponka, A., Bacharova, L., Schwartz, J., and Katsouyanni, K. (1997) Air pollution and daily admissions for chronic obstructive pulmonary disease in 6 European cities: results from the APHEA project. *Eur. Respir. J. 10*, 1064−1071.
(15) Bell, M. L., McDermott, A., Zeger, S. L., Samet, J. M., and Dominici, F. (2004) Ozone and short-term mortality in 95 US urban communities, 1987−2000. *J. Am. Med. Assoc. 292*, 2372−2378.
(16) Jerrett, M., Burnett, R. T., Pope, C. A., Ito, K., Thurston, G., Krewski, D., Shi, Y., Calle, E., and Thun, M. (2009) Long-term ozone exposure and mortality. *N. Engl. J. Med. 360*, 1085−1095.
(17) Müller, B., Seifart, C., and Barth, P. J. (1998) Effect of air pollutants on the pulmonary surfactant system. *Eur. J. Clin. Invest. 28*, 762−777.
(18) Putman, E., Liese, W., Voorhout, W. F., van Bree, L., van Golde, L. M. G., and Haagsman, H. P. (1997) Short-term ozone exposure affects the surface activity of pulmonary surfactant. *Toxicol. Appl. Pharmacol. 142*, 288−296.
(19) Lai, C. C., Yang, S. H., and Finlayson-Pitts, B. J. (1994) Interactions of monolayers of unsaturated phosphocholines with ozone at the air-water interface. *Langmuir 10*, 4637−4644.
(20) Wadia, Y., Tobias, D. J., Stafford, R., and Finlayson-Pitts, B. J. (2000) Real-time monitoring of the kinetics and gas-phase products of the reaction of ozone with an unsaturated phospholipid at the air−water interface. *Langmuir 16*, 9321−9330.
(21) Kim, H. I., Kim, H., Shin, Y. S., Beegle, L. W., Goddard, W. A., Heath, J. R., Kanik, I., and Beauchamp, J. L. (2010) Time resolved studies of interfacial reactions of ozone with pulmonary phospholipid surfactants using field induced droplet ionization mass spectrometry. *J. Phys. Chem. B 114*, 9496−9503.
(22) Thompson, K. C., Rennie, A. R., King, M. D., Hardman, S. J. O., Lucas, C. O. M., Pfrang, C., Hughes, B. R., and Hughes, A. V. (2010) Reaction of a phospholipid monolayer with gas-phase ozone at the air−water interface: measurement of surface excess and surface pressure in real time. *Langmuir 26*, 17295−17303.
(23) Thompson, K. C., Jones, S. H., Rennie, A. R., King, M. D., Ward, A. D., Hughes, B. R., Lucas, C. O. M., Campbell, R. A., and Hughes, A. V. (2013) Degradation and rearrangement of a lung surfactant lipid at the air−water interface during exposure to the pollutant gas ozone. *Langmuir 29*, 4594−4602.
(24) Kim, H. I., Kim, H., Shin, Y. S., Beegle, L. W., Jang, S. S., Neidholdt, E. L., Goddard, W. A., Heath, J. R., Kanik, I., and Beauchamp, J. L. (2010) Interfacial reactions of ozone with surfactant protein B in a model lung surfactant system. *J. Am. Chem. Soc. 132*, 2254−2263.
(25) Walther, F. J., Waring, A. J., Hernandez-Juviel, J. M., Gordon, L. M., Wang, Z., Jung, C. L., Ruchala, P., Clark, A. P., Smith, W. M., Sharma, S., and Notter, R. H. (2010) Critical structural and functional roles for the N-terminal insertion sequence in surfactant protein B analogs. *PLoS One 5*, e8672.
(26) Walther, F. J., Waring, A. J., Sherman, M. A., Zasadzinski, J. A., and Gordon, L. M. (2007) Hydrophobic surfactant proteins and their analogues. *Neonatology 91*, 303−310.
(27) Andersson, M., Curstedt, T., Jörnvall, H., and Johansson, J. (1995) An amphipathic helical motif common to tumourolytic polypeptide NK-lysin and pulmonary surfactant polypeptide SP-B. *FEBS Lett. 362*, 328−32.
(28) Vandenbussche, G., Clercx, A., Clercx, M., Curstedt, T., Johansson, J., Jörnvall, H., and Ruysschaert, J.-M. (1992) Secondary structure and orientation of the surfactant protein SP-B in a lipid environment. A Fourier transform infrared spectroscopy study. *Biochemistry 31*, 9169−9176.
(29) Olmeda, B., García-Álvarez, B., and Pérez-Gil, J. (2013) Structure-function correlations of pulmonary surfactant protein SP-B and the saposin-like family of proteins. *Eur. Biophys. J. 42*, 209−222.
(30) Gordon, L. M., Lee, K. Y., Lipp, M. M., Zasadzinski, J. A., Walther, F. J., Sherman, M. A., and Waring, A. J. (2000) Conformational mapping of the N-terminal segment of surfactant protein B in lipid using ^{13}C-enhanced Fourier transform infrared spectroscopy. *J. Pept. Res. 55*, 330−347.
(31) Kurutz, J. W., and Lee, K. Y. C. (2002) NMR structure of lung surfactant peptide SP-B(11−25). *Biochemistry 41*, 9627−9636.
(32) Booth, V., Waring, A. J., Walther, F. J., and Keough, K. M. W. (2004) NMR structures of the C-terminal segment of surfactant protein B in detergent micelles and hexafluoro-2-propanol. *Biochemistry 43*, 15187−15194.
(33) Shanmukh, S., Biswas, N., Waring, A. J., Walther, F. J., Wang, Z., Chang, Y., Notter, R. H., and Dluhy, R. A. (2005) Structure and properties of phospholipid-peptide monolayers containing monomeric SP-B_{1-25} II. Peptide conformation by infrared spectroscopy. *Biophys. Chem. 113*, 233−244.
(34) Waring, A. J., Walther, F. J., Gordon, L. M., Hernandez-Juviel, J. M., Hong, T., Sherman, M. A., Alonso, C., Alig, T., Braun, A., Bacon, D., and Zasadzinski, J. A. (2005) The role of charged amphipathic helices in the structure and function of surfactant protein B. *J. Pept. Res. 66*, 364−374.
(35) Sarker, M., Waring, A. J., Walther, F. J., Keough, K. M. W., and Booth, V. (2007) Structure of mini-B, a functional fragment of surfactant protein B, in detergent micelles. *Biochemistry 46*, 11047−11056.
(36) Fullagar, W. K., Aberdeen, K. A., Bucknall, D. G., Kroon, P. A., and Gentle, I. R. (2003) Conformational changes in SP-B as a function of surface pressure. *Biophys. J. 85*, 2624−2632.
(37) Fullagar, W. K., Holt, S. A., and Gentle, I. R. (2008) Structure of SP-B/DPPC mixed films studied by neutron reflectometry. *Biophys. J. 95*, 4829−4836.
(38) Lee, K. Y., Majewski, J., Kuhl, T. L., Howes, P. B., Kjaer, K., Lipp, M. M., Waring, A. J., Zasadzinski, J. A., and Smith, G. S. (2001) Synchrotron X-ray study of lung surfactant-specific protein SP-B in lipid monolayers. *Biophys. J. 81*, 572−585.

DOI: 10.1021/acs.biochem.5b00308
Biochemistry 2015, 54, 5185−5197

(39) Postle, A. D., Heeley, E. L., and Wilton, D. C. (2001) A comparison of the molecular species compositions of mammalian lung surfactant phospholipids. *Comp. Biochem. Physiol., Part A: Mol. Integr. Physiol. 129*, 65−73.
(40) Schägger, H. (2006) Tricine-SDS-PAGE. *Nat. Protoc. 1*, 16−22.
(41) Botchway, S. W., Parker, A. W., Bisby, R. H., and Crisostomo, A. G. (2008) Real-time cellular uptake of serotonin using fluorescence lifetime imaging with two-photon excitation. *Microsc. Res. Tech. 71*, 267−273.
(42) Stefaniu, C., and Brezesinski, G. (2014) X-Ray Investigation of Monolayers Formed at the Soft Air/Water Interface. *Curr. Opin. Colloid Interface Sci. 19*, 216−227.
(43) Fragneto, G. (2012) Neutrons and Model Membranes. *Eur. Phys. J.: Spec. Top. 213*, 327−342.
(44) Penfold, J., and Thomas, R. K. (2014) Neutron Reflectivity and Small Angle Neutron Scattering: an Introduction and Perspective on Recent Progress. *Curr. Opin. Colloid Interface Sci. 19*, 198−206.
(45) Campbell, R. A., Wacklin, H. P., Sutton, I., Cubitt, R., and Fragneto, G. (2011) FIGARO: The new horizontal neutron reflectometer at the ILL. *Eur. Phys. J. Plus 126*, 1−22.
(46) Penfold, J., Richardson, R. M., Zarbakhsh, A., Webster, J. R. P., Bucknall, D. G., Rennie, A. R., Jones, R. A. L., Cosgrove, T., Thomas, R. K., Higgins, J. S., Fletcher, P. D. I., Dickinson, E., Roser, S. J., McLure, I. A., Hillman, A. R., Richards, R. W., Staples, E. J., Burgess, A. N., Simister, E. A., and White, J. W. (1997) Recent advances in the study of chemical surfaces and interfaces by specular neutron reflection. *J. Chem. Soc., Faraday Trans. 93*, 3899−3917.
(47) Arnold, T., Nicklin, C., Rawle, J., Sutter, J., Bates, T., Nutter, B., McIntyre, G., and Burt, M. (2012) Implementation of a beam deflection system for studies of liquid interfaces on beamline I07 at Diamond. *J. Synchrotron Radiat. 19*, 408−416.
(48) Khabiri, M., Roeselova, M., and Cwiklik, L. (2012) Properties of oxidized phospholipid monolayers: an atomistic molecular dynamics study. *Chem. Phys. Lett. 519−520*, 93−99.
(49) Pryor, W. A. (1992) How Far Does Ozone Penetrate Into the Pulmonary Air/Tissue Boundary Before It Reacts? *Free Radical Biol. Med. 12*, 83−88.
(50) Enami, S., Hoffmann, M. R., and Colussi, A. J. (2009) Simultaneous detection of cysteine sulfenate, sulfinate, and sulfonate during cysteine interfacial ozonolysis. *J. Phys. Chem. B 113*, 9356−9358.
(51) Enami, S., Hoffmann, M. R., and Colussi, A. J. (2009) Ozone oxidizes glutathione to a sulfonic acid. *Chem. Res. Toxicol. 22*, 35−40.
(52) Sarker, M., Rose, J., McDonald, M., Morrow, M. R., and Booth, V. (2011) Modifications to surfactant protein B structure and lipid interactions under respiratory distress conditions: consequences of tryptophan oxidation. *Biochemistry 50*, 25−36.
(53) Kim, Y. H., Berry, A. H., Spencer, D. S., and Stites, W. E. (2001) Comparing the effect on protein stability of methionine oxidation *versus* mutagenesis: steps toward engineering oxidative resistance in proteins. *Protein Eng., Des. Sel. 14*, 343−47.
(54) Cataldo, F. (2006) Ozone degradation of biological macromolecules: proteins, hemoglobin, RNA, and DNA. *Ozone: Sci. Eng. 28*, 317−328.

DOI: 10.1021/acs.biochem.5b00308
Biochemistry 2015, 54, 5185−5197